

Solid-state and Calculated Electronic Structure of 4-Acetylpyrazole

Guido D. Frey^a, Wolfgang W. Schoeller^b and Eberhardt Herdtweck^a

^a Department Chemie, Lehrstuhl für Anorganische Chemie, Technische Universität München, Lichtenbergstraße 4, 85747 Garching, Germany

^b Fakultät für Chemie, Theoretische Chemie, Universität Bielefeld, Universitätsstraße 25, 33615 Bielefeld, Germany

Reprint requests to Dr. Guido D. Frey. Tel.: +49(0)89 289 13143. E-mail: guido.frey@ch.tum.de

Z. Naturforsch. **2014**, *69b*, 839–843 / DOI: 10.5560/ZNB.2014-4064

Received March 17, 2014

The crystal structure of 1-(1*H*-pyrazol-4-yl)ethanone (commonly known as 4-acetylpyrazole; C₅H₆N₂O) was determined from single-crystal X-ray data at 173 K: monoclinic, space group *P*2₁/*n* (no. 14), *a* = 3.865(1), *b* = 5.155(1), *c* = 26.105(8) Å, β = 91.13(1)°, *V* = 520.0(2) Å³ and *Z* = 4. The adjacent molecules assemble into a wave-like ribbon structure in the solid state, linked by strong intermolecular N–H⋯N hydrogen bonds between the pyrazole rings and a weak C–H⋯O=C hydrogen bond involving the carbonyl group. The ribbons are stacked in the solid state *via* weak π interactions between the pyrazole rings.

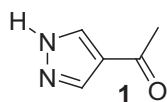
Key words: Crystal Structure, 4-Acetylpyrazole, Pyrazole

Introduction

“Standard” molecules are often used in the literature for studying the influence of hydrogen bonds in the solid state. The parent pyrazole is such a compound, which forms N–H⋯N hydrogen bonds to build up supramolecular assemblies. An N–H⋯N proton is often crystallographically disordered or even found to be shared between the nitrogen atoms. When the pyrazole derivatives have substituents at positions 3, 4 and 5 with additional donor atoms, they can form additional bridging interactions in the solid state and coordinate in several ways. An example of this can be seen in the structure of 3-amino-4-acetyl-5-methylpyrazole [1].

Results and Discussion

We report here the crystal structure of 4-acetylpyrazole (**1**), one of the simplest representatives of a substituted pyrazole with an additional donor atom, first mentioned by Wijnberger and Habraken in 1969 [2].



Compound **1** appears in nature in traces as a side-product in roasted sesame seed oil [3, 4] or roasted chicory root [5], which can be used as a substitute for coffee and as a tobacco flavor ingredient [6]. Compound **1** can also be found in small amounts in dried red pepper [7]. During the typical La Vera drying process [8] of red pepper, the amount of compound **1** by weight can be increased over time. During the fermentation process of sausages compound **1** is also formed in small amounts as a decomposition product of fatty acids and the Strecker products of amino acids [9, 10].

We prepared 4-acetylpyrazole (**1**) according to the procedure by Birkofer and Franz [11] *via* the reaction of 4-trimethylsilyl-but-3-yn-2-one [12] and diazomethane. After neutralization with caustic soda during the work-up procedure, extraction and removal of the solvent we obtained a colorless precipitate, which was recrystallized from chloroform. Analytical data (¹H NMR, IR (CHCl₃), EA, MS [13], and melting point [14]) were in accordance with those found in the literature [11, 15].

Suitable single crystals for X-ray diffraction studies were grown from a saturated chloroform solution by slow evaporation of the solvent at room temperature. A view of the low-temperature (173 K) molecular structure of compound **1** is given in Fig. 1. Selected ge-

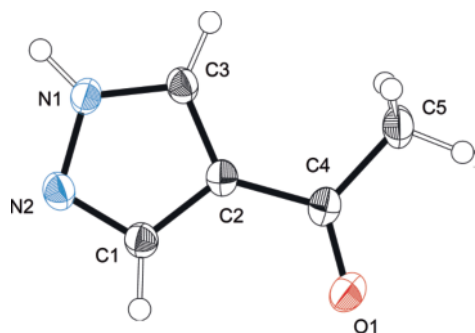


Fig. 1. An ORTEP [16] plot of compound **1** in the solid state showing 50% probability displacement ellipsoids and the atom numbering scheme.

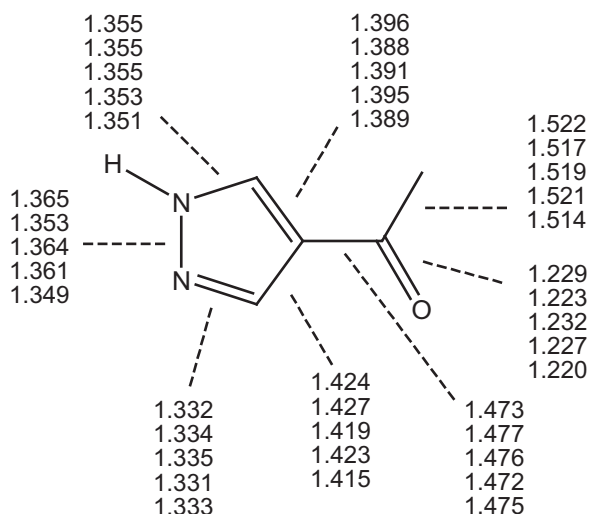


Fig. 2. Structural parameters of monomeric **1** at different levels of computational sophistication. Numbers from top to bottom: RI-BP86(D)/TZVP; RI-MP2(fc)-SCS/TZVP; RI-CC2(fc)/TZVP; RI-BP86(D)/TZVPP; RI-MP2(fc)-SCS/TZVPP.

ometric and structural parameters are listed in Tables 1 and 2.

In order to gain deeper insight into the bonding in **1**, quantum-chemical calculations at density functional (RI-BP86(D)) as well as *ab-initio* level of sophistication (RI-MP2(fc)-SCS) were performed with the TURBOMOLE 6.2 set of program systems [17]. Basis sets of triple-zeta quality with one (TZVP) or two sets of polarization functions (TZVPP) were utilized, in order to account for the (relatively) weak hydrogen bonding in these systems. More computational details are given in the Experimental Section of this publication.

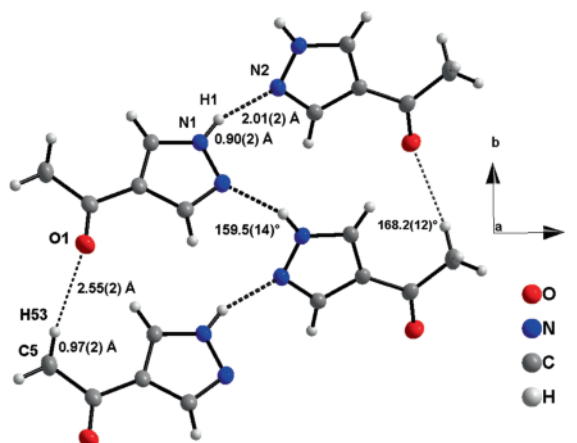


Fig. 3. DIAMOND [20] plot of the crystal structure of compound **1** as viewed down the crystallographic *a* axis. Dotted lines show the N–H...N as well as the C=O...H interactions.

Table 1. Selected bond lengths (Å) and bond angles (deg) for compound **1** in the solid state. Numbers in brackets are the theoretical values of the calculations (RI-MP2(fc)-SCS/TZVPP).

O1–C4	1.222(2) [1.220]	N2–N1–C3	112.3(1) [113.60]
N1–C3	1.338(2) [1.351]	N1–N2–C1	104.8(1) [104.06]
N1–N2	1.358(2) [1.349]	N2–C1–C2	111.6(1) [111.93]
N2–C1	1.324(2) [1.333]	C1–C2–C3	104.38(9) [104.33]
C1–C2	1.405(2) [1.415]	C3–C2–C4	128.9(1) [128.80]
C2–C3	1.385(2) [1.389]	C1–C2–C4	126.8(1) [126.87]
C2–C4	1.469(2) [1.475]	N1–C3–C2	107.0(1) [106.09]
C4–C5	1.496(2) [1.514]	O1–C4–C2	120.8(1) [121.01]
		O1–C4–C5	122.0(1) [121.81]
		C2–C4–C5	117.2(1) [117.18]

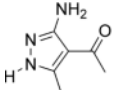
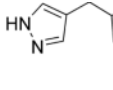
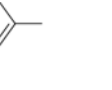
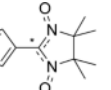
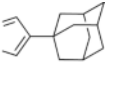
Table 2. Hydrogen bond geometry (Å, deg) of compound **1** in the solid state^a. Numbers in brackets are the theoretical values derived from DFT calculations (RI-BP86(D)/TZVP) for a hexameric unit.

D–H...A	D–H	H...A	D...A	D–H...A
C5–H53...O1 ⁱ	0.97(2)	2.55(3)	3.51(2)	168.2(12)
	[1.10]	[2.52–2.55]	[~ 3.55]	[152–154]
N1–H1...N2 ⁱⁱ	0.90(2)	2.01(2)	2.867(2)	159.5(14)
	[~ 1.045]	[~ 1.82]	[~ 2.82]	[159–161]
C2...C3 ⁱⁱⁱ	–	–	3.387(2)	–

^a Symmetry operation for equivalent atoms (i): $x, 1+y, z$; (ii): $2.5-x, 0.5+y, 0.5-z$; (iii): $-1+x, y, z$.

The structure of monomeric **1** was studied initially. The bond lengths computed using different levels of sophistication are summarized in Fig. 2. Throughout these studies, similar bond lengths for monomeric **1** were found.

Table 3. Comparison of bond lengths (Å) of similar pyrazoles.

						
	1	2 [1]	3 [19]	4 [18]	5 [21]	6 [22]
N1–N2	1.358(2)	1.378(2)	1.347–1.360	1.343–1.349	1.346(2)	1.327
N1–C3	1.338(2)	1.331(3)	1.341–1.343	1.344–1.345	1.335(2)	1.353
N2–C1	1.324(2)	1.328(3)	1.333–1.335	1.338–1.339	1.318(2)	1.323
C1–C2	1.405(2)	1.431(4)	1.395–1.401	1.393–1.400	1.405(2)	1.405
C2–C3	1.385(2)	1.401(3)	1.369–1.379	1.377–1.391	1.373(2)	1.370
O1–C4	1.222(2)	1.237(3)	–	–	–	–
C2–C4	1.469(2)	1.438(4)	–	–	–	–
C4–C5	1.496(2)	1.505(4)	–	–	–	–

The DFT calculations (RI-BP86(D)/TZVP) show only small variations in bond lengths and bond angles when compared to the more sophisticated *ab initio* calculations (RI-MP2(fc)-SCS/TZVPP), and compare well with experimental values. The deviations might be the result of the strong intermolecular interactions in the solid phase compared to the single molecule in the gas phase. The experimentally determined bond lengths and angles in the solid-state structure are in good agreement with other solid-state structures of pyrazole derivatives (Table 3). As in the experimental crystal structure the calculated one is dominated by two strong intermolecular N–H...N hydrogen bond interactions (see Table 2), forming a ribbon arrangement. The intermolecular hydrogen-nitrogen distance (2.01(2) Å) is within the normal range (2.02(5) Å) [18, 19]. The twisted structure is linked by another very weak hydrogen interaction (2.55(2) Å) of the methyl group from one molecule with the oxygen of the carbonyl group to form a one-dimensional framework. This simple dimensionality may be a result of the very strong N–H...N bond formation for dimers and the lack of presence of other atoms for the formation of hydrogen bonding.

As is shown in Fig. 3, these hydrogen bonds combine to assemble an infinite wave-like ribbon structure running parallel to the crystallographic *b* axis. The stacking of the different ribbons in the solid state results from very weak interactions between the π systems of the heterocycles, resulting *inter alia* in an interaction (3.387(2) Å) between C2 in one ribbon and C3 in the next one (see Table 2). Adjacent individual ribbons, and hence the stacks of these ribbons, are orientated in the solid state by a 180° rotation with respect

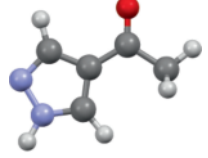
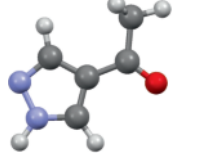
to each other with no significant hydrogen-bonding interactions in between.

In order to mimic the bonding in the crystal we optimized a layer framework of six molecules, connected *via* π stacking (RI-BP86(D)/TZVP level). The averaged calculated torsion angle O1–C4–C2–C1 is 0.35°, as compared with 0.2(2)° observed in the experiment. Thus theory and experiment are in accord with each other.

As we had used the experimental geometry of **1** and its observed conformation as the starting point of the DFT calculations, we were also interested in studying the other possible conformer, in which the acetyl group is rotated by 180°, and the C=O unit points towards the NH group of the pyrazole ring. Compound **1a** has a 0.69 kcal/mol lower energy minimum than compound **1** (Table 4).

In a second step we probed also a hexamer of **1** by DFT calculations using the RI-B86(D)/(TZVP) computational level. In this framework the experimental bond lengths and bond angles are in better agreement with the experimental solid-state structure, compared

Table 4. Relative energies (in kcal mol⁻¹) for the different conformers of compound **1** at the RI-BP-86-D/TZVP computational level.

		
Compound	1	1a
E_{rel} , kcal mol ⁻¹	+0.69	0

to the single molecule calculated by DFT calculations (as shown in brackets in Table 1). The intermolecular distances between the molecules, shown in Table 2 in brackets, are also in relatively good agreement with the solid-state structure for such a calculated small unit.

Experimental Section

Synthesis

Compound **1** was prepared with an overall yield of 93% analogous to the procedure reported by Birkofer and Franz [11]. M. p. 113–115 °C. – IR (CHCl₃): $\nu = 3443$ (N–H), 1673 (C=O) cm⁻¹. – ¹H NMR (300 MHz, CDCl₃): $\delta = 11.3$ (br, 1 H, NH), 8.13 (s, 2 H, CH), 2.47 ppm (s, 3 H,

CH₃). – MS (EI, 70 eV): $m/z(\%) = 111$ (5) [M+H]⁺, 110 (35) [M]⁺, 96 (8), 95 (100), 68 (48), 67 (12), 43 (47), 40 (32). – C₅H₆N₂O (110.12): calcd. C 54.54, H 5.49, N 25.44; found C 54.49, H 5.43, N 25.27.

Single-crystal X-ray structure determination of compound **1**

Suitable single crystals for the X-ray diffraction study were grown from chloroform. Crystal data and details of the structure determination are presented in Table 5.

The crystal was fixed on the top of a glass fiber with perfluorinated ether and transferred into a Lindemann capillary for data collection. The intensity data were corrected for Lorentz, polarization effects and a decay of 3.3%. The structure was solved by a combination of Direct Methods and difference Fourier syntheses [23]. All non-hydrogen atoms were refined with anisotropic displacement parameters. All hydrogen atoms were found in the final difference Fourier maps and allowed to refine freely with isotropic displacement parameters. Full-matrix least-squares refinements with 97 parameters were carried out by minimizing $\sum w(F_o^2 - F_c^2)^2$ with the SHELXL-97 [24–26] weighting scheme and stopped at a shift over error ratio of < 0.001.

CCDC 992137 contains the supplementary crystallographic data for this paper. These data can be obtained free of charge from The Cambridge Crystallographic Data Centre via www.ccdc.cam.ac.uk/data_request/cif.

Calculations

All calculations were performed with the TURBOMOLE program systems in the version 6.2 [17]. The resolution of the identity (RI) based on the BP86 functional [27, 28] was used in combination with the TZVP basis set (TZV basis set of triple- ξ quality plus one set of *p* functions at the hydrogens plus one set of *d* functions for all other atoms) [29]. Alternatively the more flexible TZVPP basis contains two sets of polarization functions. The density functional calculations were at times corrected for dispersion interactions (D) utilizing the Grimme approach [30].

Acknowledgement

E. H. thanks the Lehrstuhl für Anorganische Chemie of the Technische Universität München for X-ray facility support.

Table 5. Summary of the crystallographic data of compound **1**.

Empirical formula	C ₅ H ₆ N ₂ O
Molecular weight	110.12
Crystal color/shape	colorless/needle
Crystal size, mm ³	0.10 × 0.15 × 0.81
Crystal system	monoclinic
Space group	<i>P</i> 2 ₁ / <i>n</i> (no. 14)
<i>a</i> , Å	3.865(1)
<i>b</i> , Å	5.155(1)
<i>c</i> , Å	26.105(8)
β , deg	91.13(1)
<i>V</i> , Å ³	520.0(2)
<i>Z</i>	4
$\rho_{\text{calcd.}}$, g cm ⁻³	1.41
μ , mm ⁻¹	0.1
Wavelength; λ , Å	MoK α ; 0.71073
<i>T</i> , K	173(1)
Θ range, deg	1.56–25.98
Reflections integrated	2219
Independent reflections (all data)/ <i>R</i> _{int}	1020/0.013
Observed reflections [<i>I</i> > 2 σ (<i>I</i>)]	870
Parameters refined	97
<i>R</i> 1 (observed/all data) ^a	0.0304/0.0387
<i>wR</i> 2 (observed/all data) ^b	0.0774/0.0817
GOF ^c	1.068
Largest diff. peak/hole, e Å ⁻³	0.23/–0.20

^a $R1 = \sum ||F_o| - |F_c|| / \sum |F_o|$; ^b $wR2 = [\sum w(F_o^2 - F_c^2)^2 / \sum w(F_o^2)]^{1/2}$, $w = [\sigma^2(F_o^2) + (AP)^2 + BP]^{-1}$, where $P = (\text{Max}(F_o^2, 0) + 2F_c^2)/3$; ^c $\text{GoF} = [\sum w(F_o^2 - F_c^2)^2 / (n_{\text{obs}} - n_{\text{param}})]^{1/2}$.

- [1] A. Hergold-Brundić, B. Kaitner, B. Kamenar, V. M. Leovac, E. Z. Ivegeš, N. Juranić, *Inorg. Chim. Acta* **1991**, *188*, 151–158.
- [2] C. Wijnberger, C. L. Habraken, *J. Heterocycl. Chem.* **1969**, *6*, 545–551.
- [3] M. Shimoda, Y. Nakada, M. Nakashima, Y. Osajima, *Food Sci. Technol. Int.* **1998**, *4*, 14–17.
- [4] M. Shimoda, H. Shiratsuchi, Y. Nakada, Y. Wu, Y. Osajima, *J. Agric. Food Chem.* **1996**, *44*, 3909–3912.

- [5] A. Sannai, T. Fujimori, K. Kato, *Agric. Biol. Chem.* **1982**, *46*, 429–433.
- [6] K. R. Kim, A. Zlatkis, J. W. Park, U. C. Lee, *Chromatographia* **1982**, *15*, 559–563.
- [7] M. C. V. Aragon, M. Lozano, V. M. De Espinosa, *J. Food Qual.* **2005**, *28*, 211–221.
- [8] M. Lozano, V. M. De Espinosa, *Alimentaria* **1999**, *300*, 91–99.
- [9] G. Johansson, J.-L. Berdague, M. Larsson, N. Tran, E. Borch, *Meat Sci.* **1994**, *38*, 203–218.
- [10] H. V. Ba, T. Amna, I. Hwang, *Meat Sci.* **2013**, *94*, 480–488.
- [11] L. Birkofer, M. Franz, *Chem. Ber.* **1972**, *105*, 1759–1767. A more detailed procedure can be found in: G. Heinisch, W. Holzer, C. Obala, *Monatsh. Chem.* **1988**, *119*, 253–262.
- [12] L. Birkofer, A. Ritter, H. Uhlenbrauck, *Chem. Ber.* **1963**, *96*, 3280–3288.
- [13] J. Van Thuijl, K. J. Klebe, J. J. Van Houte, *Org. Mass Spect.* **1970**, *3*, 1549–1559.
- [14] E. Zbiral, E. Bauer, *Tetrahedron* **1972**, *28*, 4189–4196.
- [15] M. Braun, G. Buechi, D. F. Bushey, *J. Am. Chem. Soc.* **1978**, *100*, 4208–4213.
- [16] A. L. Spek, PLATON, A Multipurpose Crystallographic Tool, Utrecht University, Utrecht (The Netherlands) **2010**.
- [17] F. Furche, R. Ahlrichs, C. Hättig, W. Klopper, M. Sierka, F. Weigend, *WIREs Comput. Mol. Sci.* **2014**, *4*, 91–100.
- [18] R. Goddard, R. M. Claramunt, C. Escolástico, J. Elguero, *New J. Chem.* **1999**, *23*, 237–240.
- [19] M. A. Monge, E. G. Pugebla, J. Elguero, C. Toiron, W. Meutermaans, I. Sobrados, *Spectrochim. Acta, Part A* **1994**, *50*, 727–734.
- [20] K. Brandenburg, DIAMOND (version 3.2i), Crystal and Molecular Structure Visualization, Crystal Impact – H. Putz & K. Brandenburg GbR, Bonn (Germany) **2012**.
- [21] L. Catala, K. Wurst, D. B. Amabilino, J. Veciana, *J. Mater. Chem.* **2006**, *16*, 2736–2745.
- [22] P. Cabildo, R. M. Claramunt, I. Forfar, C. Foces-Foces, A. L. Llamas-Saiz, J. Elguero, *Heterocycles* **1994**, *37*, 1623–1636.
- [23] A. Altomare, G. Cascarano, C. Giacovazzo, A. Guagliardi, M. C. Burla, G. Polidori, M. Camalli, *J. Appl. Cryst.* **1994**, *27*, 435–436.
- [24] G. M. Sheldrick, SHELXL-97, Program for the Refinement of Crystal Structures, University of Göttingen, Göttingen (Germany) **1998**.
- [25] L. J. Farrugia, WINGX (version 1.80.05), A MS-Windows System of Programs for Solving, Refining and Analysing Single Crystal X-ray Diffraction Data for Small Molecules, University of Glasgow, Glasgow, Scotland (U. K.) **2011**.
- [26] L. J. Farrugia, *J. Appl. Cryst.* **1999**, *32*, 837–838.
- [27] A. D. Becke, *Phys. Rev. A* **1988**, *38*, 3098–3100.
- [28] J. Perdew, *Phys. Rev. B* **1986**, *33*, 8822–8824.
- [29] A. Schäfer, C. Huber, R. Ahlrichs, *J. Chem. Phys.* **1994**, *100*, 5829–5835.
- [30] S. Grimme, *J. Comput. Chem.* **2006**, *27*, 1787–1799.